

# Wireless Structural Health Monitoring of Wind Turbine Blades Using an Energy Harvester as a Sensor

Dong-Won Lim, Susan C. Mantell, and Peter J. Seiler  
University of Minnesota, Minneapolis, MN, 55455

Structural Health Monitoring (SHM) of wind turbine blades is critical to improve the reliability of wind turbines. A health monitoring algorithm was developed that utilizes energy harvesters as sensors. An *accumulated energy sensor* is described in which an energy harvester mounted on the surface of the wind turbine blade converts low frequency vibrational strain energy from the blade to electrical charge, that is subsequently stored to power an RF transmitter. The premise of this sensing approach is that the timing of data output from the RF transmitter, which is tied to the charging time, is indicative of the structural health. The time between data transmission pulses will be reduced if the blade stiffness decreases. The SHM algorithm compares data transmission time for the three blades to identify the onset of blade damage. To demonstrate the effectiveness of the algorithm, an expected energy harvester signal transmission rate is established from blade strain data from a 2.5 MW wind turbine. The transmission rates for the three blades are compared to establish a threshold for “healthy” blades. Simulated damage corresponding to approximately 20% increase in harvested energy can be detected by the SHM algorithm.

## Nomenclature

$E$	=	Young’s Modulus of an EH, GPa ( $E_0 = 1$ GPa)
$K_{EH}$	=	EH design factor, $m^3$
$P_{avail}$	=	Available strain power density, $W/m^3$
$R_{i-j}$	=	Pulse timing ratio between blades $i$ and $j$
$T$	=	Failure detection threshold
$V$	=	Volume of an EH, $m^3$
$W_{EH}$	=	Harvested strain energy, J
$f$	=	Strain frequency, Hz
$g_D$	=	Damage factor
$n$	=	cycles of excitations
$\Delta t$	=	Discretization step time, sec
$\delta t$	=	Charging time, sec
$w_{in}$	=	Input strain energy density, $J/m^3$
$\varepsilon$	=	Mechanical strain, $\mu\text{-}\varepsilon$
$\varepsilon_a$	=	Mechanical strain amplitude (mean-peak), $\mu\text{-}\varepsilon$
$\eta$	=	Energy conversion efficiency
$\psi_{i-j}$	=	Pulse timing ration deviation by damage of $R_{i,j}$

## I. Introduction

THE DOE has set a goal of “20% wind energy by 2030”.<sup>1</sup> Reduction in operating and maintenance costs for wind turbines has been identified as a major challenge to achieving this goal. Wind turbine maintenance is a particular challenge because wind turbines are often located in remote regions (including offshore). Structural Health Monitoring (SHM) is a promising approach that can enable preventative maintenance, reduce down time and significantly reduce life-cycle costs.<sup>2</sup> While failure can occur in any structural component, one of the most common and critical components to fail is the wind turbine blade.<sup>3</sup> It is particularly challenging to continuously monitor blade

health: (1) the blades are quite long and an extensive network of sensors is required; and (2) the blades are rotating, posing challenges to delivering power to and receiving data from the sensor network.

A novel sensing and SHM system is proposed. The system is comprised of a network of discrete sensor nodes. Each wireless node includes an energy harvester to convert vibrational strain energy from the blade to electrical charge and an RF transmitter circuit. The electrical charge from the energy harvester is stored to power an RF transmitter. The RF transmitter wirelessly communicates a single pulse to a centralized monitoring system in the turbine nacelle when sufficient electrical charge has been stored. The premise of this sensing approach is that the timing of data output from the RF transmitter, which is tied to the charging time, is indicative of the structural health. In a damaged blade, changes in the stiffness (associated with damage) will lead to a change in blade strain<sup>4</sup>, resulting in a change in the timing of the RF pulses.

To demonstrate the effectiveness of the proposed sensor-algorithm, a study is presented that utilizes blade strain data from the Eolos 2.5 MW wind turbine installed at the University of Minnesota. Fiber optic strain sensors were installed at several locations on each of the three blades of the Eolos turbine. At this stage of the research, energy harvesters have not yet been installed on the turbine blades. Hence, the low frequency strain data are converted to *simulated* energy harvester pulse transmission data. These simulated energy harvester data are the basis for evaluation of the health monitoring algorithm.

## II. Background

### A. Health Monitoring of Wind Turbine Blades

Structural health monitoring<sup>5</sup> is the process of implementing a damage detection strategy for an engineering structure. SHM algorithms have been well-studied because structural damage can have significant safety impacts. The literature on SHM includes many applications to wind turbine blades.<sup>2,5-13</sup> Methods include acoustic emission, thermal imaging, ultrasonic methods, modal approaches, fiber optic methods, laser Doppler, electrical resistance, and X-rays<sup>9</sup>. Vibration-based SHM methods<sup>5,11</sup> seem most appropriate for the proposed architecture. Vibration-based SHM can be largely categorized into frequency/modal domain and time domain analysis. Some of the previous work in this area is briefly reviewed. NASA<sup>14</sup> developed an impedance-based SHM system by PZT sensors and actuators. The SHM system can detect damage inside a blade but a sensor must be placed close to the damage. Pitchford et al.<sup>13</sup> also studied impedance-based SHM using MFC piezoelectric materials. While modal testing, MFC patches are used for monitoring material behavior with an active impedance method. Ghoshal et al.<sup>2</sup> presented four blade health monitoring techniques: transmittance functions, ODS, resonant comparison, and wave propagation. The feasibility to detect damage was indicated by using piezoceramic patches for excitation and a scanning laser Doppler vibrometer or piezoceramic patches to measure vibration. Shulz<sup>10</sup> suggested a smart sensor system to actively detect a fault in a composite blade. White et al.<sup>6</sup> presented a SHM method for a lab-scale carbon composite wind turbine blade, TX-100. In this paper, several accelerometers were deployed and they used virtual forces, transmissibility, and time-frequency analysis. In Ref. 8, their methods were shown as not effective on damage detection located farther than 2 meters from a sensor. Rumsey et al.<sup>8</sup> studied a few direct measuring methods based on strain gages and acoustic emission sensors. They concluded unique sound events were captured when damage occurred and strain energy reduction over fatigue cycles was observed as damage increased.

In summary, there is a large body of work on SHM for wind turbine blades. Most of these techniques employ a small number of sensors to detect structural damage. The use of energy harvesting sensors with wireless communication eliminates the need for costly wiring which requires maintenance. As a result, it is feasible to implement an array of many sensors on each of the three turbine blades.

### B. Energy Harvester as a Sensor

It is important to estimate the strain energy available for powering SHM sensors. The strain energy density  $w_{strain}$  (J/m<sup>3</sup>) at a given strain  $\epsilon_1$  (unitless) is given by the fundamental equation:

$$w_{strain} = \int_0^{\epsilon_1} \sigma d\epsilon \quad (1)$$

where  $\sigma$  is the stress (Pa). If the Young's modulus  $E$  (GPa) is constant then the strain energy density (J/m<sup>3</sup>) can be expressed entirely in terms of strain as

$$w_{strain} = \int_0^{\epsilon_1} E \epsilon d\epsilon . \quad (2)$$

This relation provides the strain energy density at a given strain  $\epsilon_1$ . An EH, when subjected to time-varying strains, converts a fraction of the mechanical strain energy input into usable electrical energy. The EH efficiency  $\eta$

(unitless) is defined as the energy conversion ratio from mechanical input to electrical energy output. This efficiency is typically on the order of  $10^{-2}$ . Assuming  $\eta$  is known, the harvested energy is estimated by the input energy multiplied by  $\eta$ . External forces are converted to electric energy when the EH is stretched or compressed. The input energy is calculated from strain by considering only conditions when the strain  $\varepsilon(t)$  and the strain rate  $\dot{\varepsilon}(t)$  are the same sign. Thus the total input energy density  $w_{in}$  to the harvester is given by

$$w_{in} = \int_0^{t_1} w_{instant}(\varepsilon(t), \dot{\varepsilon}(t)) dt \quad (3)$$

where the instantaneous energy density  $w_{instant}$  is

$$w_{instant}(\varepsilon, \dot{\varepsilon}) = \begin{cases} E\varepsilon\dot{\varepsilon} & \text{if } \varepsilon\dot{\varepsilon} > 0 \\ 0 & \text{else.} \end{cases} \quad (4)$$

Explicit formulas for the harvested energy can be derived if the strain is sinusoidal with frequency  $f$  (Hz) and peak amplitude (mean to peak) of the strain  $\varepsilon_a$  (unitless) (see **Eq. (A4)** in the Appendix). For example, if  $\varepsilon(t) = \varepsilon_a \sin(2\pi ft)$ , then the harvested energy density is

$$w_{EH} = \eta E \cdot \varepsilon_a^2 f \cdot \delta t. \quad (5)$$

The harvested energy density  $w_{EH}$  can be converted to a total harvested energy  $W_{EH}$  (J) by multiplying the volume  $V$  ( $m^3$ ) of the EH

$$W_{EH} = \eta V E \cdot \varepsilon_a^2 f \cdot \delta t. \quad (6)$$

The charging time  $\delta t$  (second) is the time required to charge the capacitor (part of the RF circuit) and will also define the time between bursts of data transmission/acquisition. The magnitude of strain and frequency will depend on the wind turbine blade geometry and operating conditions.

As noted, the energy available for harvesting depends on the strain and the frequency of vibration; and harvesting capability depends on the type and the design of an EH (**Eq. (6)**). Thus it is useful to define the power available  $P_{avail}$  ( $W/m^3$ ) and the EH design factor  $K_{EH}$  ( $m^3$ ) as

$$P_{avail} = E_0 \varepsilon_a^2 f, \quad (7)$$

$$K_{EH} = \eta V \frac{E}{E_0} \quad (8)$$

where  $E_0$  is the nominal modulus of an EH material (GPa). These definitions separate the design properties of a given EH (given in volumetric units) from the conditions in which the EH operates as specified by the power density  $P_{avail}$ . By using this measure of available power, simulation strain data can be compared for various turbines and under various operating conditions. For the purpose of comparison, a modulus of  $E_0 = 1$  GPa is taken in all plots and data reported herein. Values can easily be scaled to evaluate other harvester materials. In summary, the harvested energy can be decomposed into an internal factor ( $K_{EH}$ ) and external source ( $P_{avail}$ ) and charging time  $\delta t$ . **Eq. (6)** is simplified as

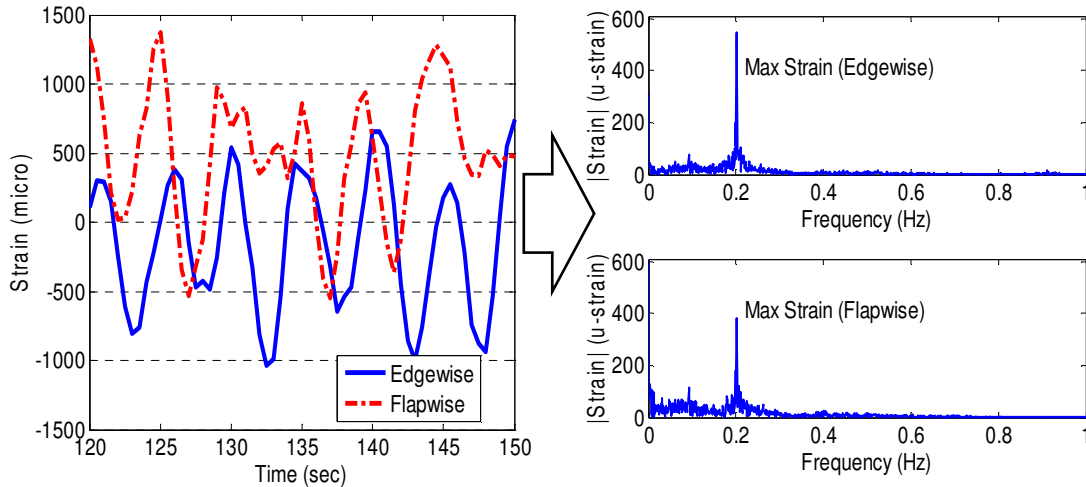


**Figure 1. Strain vs. Time at 15.9 m from hub (L) and Single sided amplitude spectrum in frequency of each flexing mode (R): Data shown for NREL offshore turbine at 24 m/s wind speed and low turbulence.**

$$W_{EH} = K_{EH} \cdot P_{avail} \cdot \delta t. \quad (9)$$

When using the energy harvester as a sensor, the energy available from harvested  $W_{EH}$  must be sufficient to charge the capacitor in the RF circuit  $W_{RF}$ . The energy required to send a single tone burst  $W_{RF}$  is set by the RF circuit/capacitor configuration, and is a fixed amount on the order of micro Joules. In this configuration, the charging time  $\delta t$  is also the time between transmission pulses. Thus, because the energy required to send a single pulse is fixed, the charging time (and time between pulses)  $\delta t$  is reduced when the power available  $P_{avail}$  increases.

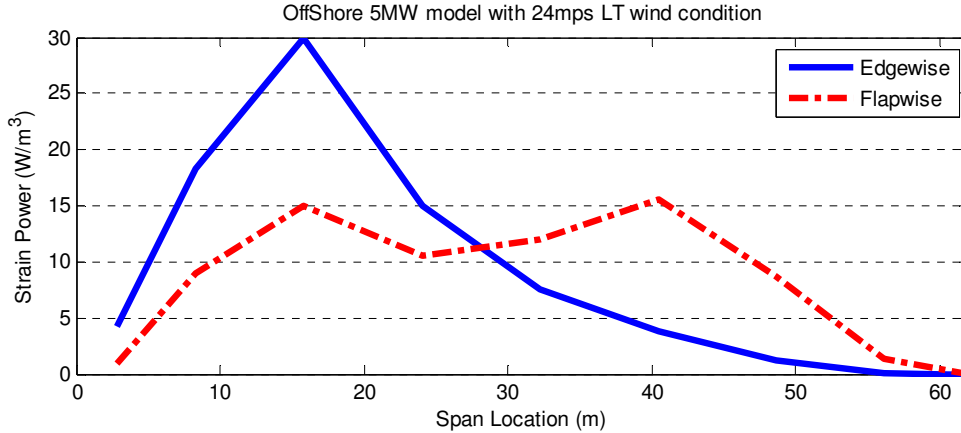


**Figure 2. Edge/Flapwise strain power available in an offshore blade as a function of blade location. Data are obtained during operational cycles corresponding to the maximum peak amplitude. ( $E_0 = 1$  GPa)**

### C. Available Strain Energy

In our earlier work<sup>15</sup>, the strain energy available was estimated for three wind turbines (a CART3 600 kW, a WindPact 1.5 MW and a 5MW offshore wind turbine) and various wind conditions (6 to 24 m/s at high and low turbulence). For the range of wind turbine sizes and wind conditions considered, the  $P_{avail}$  ranges from 1 to 30 W/m<sup>3</sup>. FAST<sup>16</sup> simulation results for the 5MW NREL offshore wind turbine operating under wind conditions of 24 m/s at low turbulence are shown in **Figure 1**. **Figure 1** shows strain data in both edgewise and flapwise bending over a 30sec time window at a location 15.9m from the rotor hub (left). Fast Fourier Transforms computed for each bending mode over a longer time window are also shown (right). As shown in

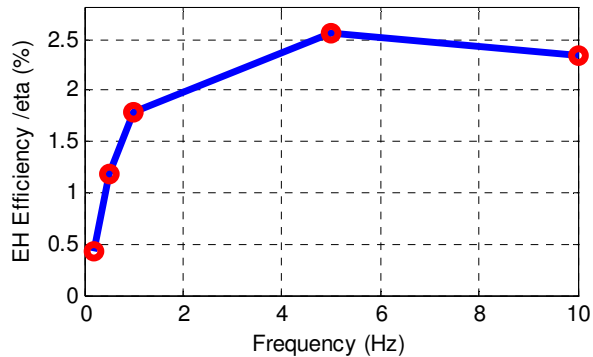


**Figure 3 Experimental result of EH conversion efficiency over input frequency (200 kΩ load resistance and 200 με input peak amplitude)**

**Figure 1**, the peak amplitude of the edgewise strain is ~550 micro-strain and the amplitude of the flapwise strain is ~390 micro-strain. These edgewise and flapwise strains are used as RMS amplitudes of ~390 and ~280 micro-strain respectively in determining the power available for the energy harvester. The strain varies with time at a periodic rate of ~0.2 Hz, corresponding to the rotational frequency of the turbine at these wind conditions. **Figure 2** shows the corresponding maximum edgewise and flapwise  $P_{avail}$  (calculated from **Eq. (7)**) along the span of the blade. The maximum edgewise  $P_{avail}$ , ~30 W/m<sup>3</sup>, occurs at a distance 15.9 m from the blade support (at the nacelle). The flapwise  $P_{avail}$  has two peaks, 15 W/m<sup>3</sup> at 15.9 M. and 16 W/m<sup>3</sup> at 40.5 m. This profile of  $P_{avail}$  along the blade length is typical for the wind turbine sizes and wind conditions considered.

In this study, a data transmission energy requirement  $W_{RF}$  of 92.4 μJ was selected, corresponding to the power requirement to transmit a signal to a data acquisition board (DAQ) in the nacelle via a commercially available wireless transmission module (EH-link from Microstrain<sup>17</sup>). The EH design factor  $K_{EH}$  is experimentally evaluated for an off the shelf energy harvester, the Smart Materials<sup>18</sup> M2814P2 type MFC with a surface area of 28 mm × 14 mm by 0.3 mm thick. The material modulus  $E$  is 30.34 GPa. It is well known that the piezo-electric EH

performance depends on the load resistance, input amplitude and frequency. Thus, the energy harvester efficiency was determined under conditions that are expected for wind turbine applications. **Figure 3** shows energy harvester efficiency  $\eta$  for tests performed at  $200 \mu\text{e}$  of input peak amplitude over frequencies ranging from 0.2 to 10 Hz. At 0.2 Hz, the energy harvester efficiency is approximately 0.4%. Under these conditions,  $K_{EH}$  is  $14.27 \text{ mm}^3$ . Given the power requirement for a single pulse ( $W_{RF} = W_{EH} = 92.4 \mu\text{J}$ ), the charging time when  $P_{avail} = 30 \text{ W/m}^3$  is 3.6 minutes.

### III. Approach

In this section, a health monitoring algorithm for detecting blade damage is described. An overview of the approach is illustrated in **Figure 4**. EHs are installed at the same locations on the three blades. From blade vibrations (first row in **Figure 4**), EHs accumulate strain energy (second row). When the accumulated strain energy is sufficient for transmitting a single data pulse, the transmitted signal is received by the DAQ system and the time is recorded (third row). The time intervals for each of the three EH pulse transmissions are compared to each other. The SHM algorithm determines whether a wind turbine blade is damaged based on the difference in the pulse timing interval among the three EHs. EHs can be installed at many locations on each blade and this monitoring algorithm can be repeated for each set of three measurements obtained from the same blade location. This enables detection of the damage location.

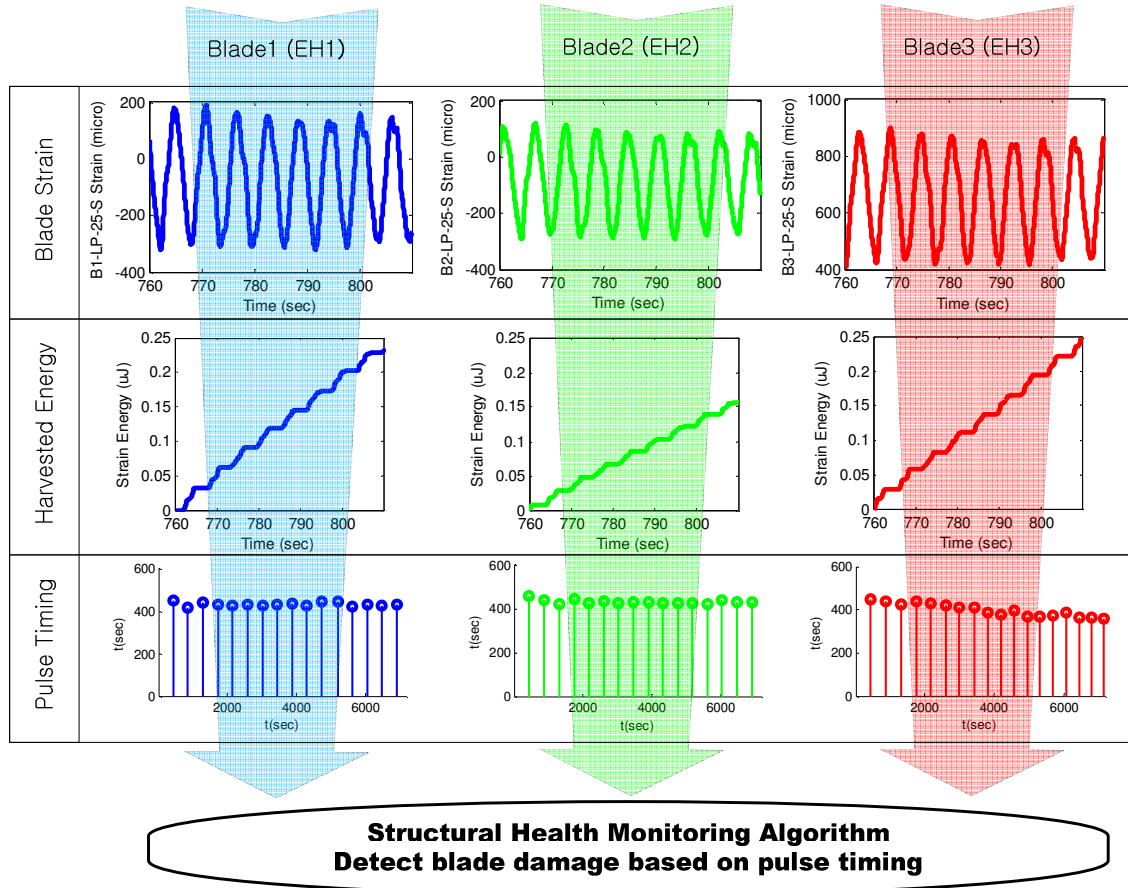


**Figure 4 Construction of Model-free Structural Health Monitoring for Wind Turbine Blades**

#### A. Damage Model

Matrix cracking is common in composite materials and initiated by multiple factors including fatigue loading. As shown in **Figure 5** (left), the stiffness decreases as the crack density increases. Thus, matrix cracking is modeled as a loss in stiffness.<sup>19</sup> A local loss in stiffness will increase the strain (and subsequently  $P_{avail}$ ) at that location. As the blade is cyclically loaded, damage will accumulate. A simple damage model of matrix cracking is shown in **Figure 5** (right) as a function of the number of loading cycles. This model introduces the concept of a damage factor  $g_D$  that tracks the stages of matrix crack growth as the part is cyclically loaded. The damage factor is initially  $g_D=1$ , corresponding to no damage, and increases to  $g_D=1.2$  corresponding to a 20% increase in strain (or 20% loss

in stiffness). Because the strain energy harvested will increase with damage, **Eq. (3)** is modified to account for the damage that accumulates with each cyclic load.

$$w_{in} = \int_0^{t_1} g_D(t) \cdot w_{instant}(\varepsilon(t), \dot{\varepsilon}(t)) dt. \quad (10)$$

This integral relation is more general than **Eq. (6)** in that it includes the factor  $g_D$  (unitless) to model damage. **Eq. (10)** can be discretized with a step size of  $\Delta t$  (sec) to accommodate an arbitrary strain profile:

$$w_{in} \approx \sum_{k=1}^n g_{D,k} \cdot w_{instant,k} \cdot \Delta t \quad (11)$$

where

$$w_{instant,k} = \begin{cases} E\varepsilon(t_k) \cdot \frac{(\varepsilon(t_k) - \varepsilon(t_{k-1}))}{\Delta t} & \text{if } \varepsilon(t_k) \cdot (\varepsilon(t_k) - \varepsilon(t_{k-1})) > 0 \\ 0 & \text{else.} \end{cases} \quad (12)$$

The total harvested strain energy given the volume of the EH  $V$  and the efficiency  $\eta$  is

$$W_{EH} \approx \eta V \sum_{k=1}^n g_{D,k} \cdot w_{instant,k} \cdot \Delta t. \quad (13)$$

**Eq. (13)** applies for more general strain conditions and not simply for single harmonic vibrations as considered in **Eq. (6)**. The discrete-summation is used to approximate the continuous integral in the simulations and this allows for the damage factor to change with each cycle.

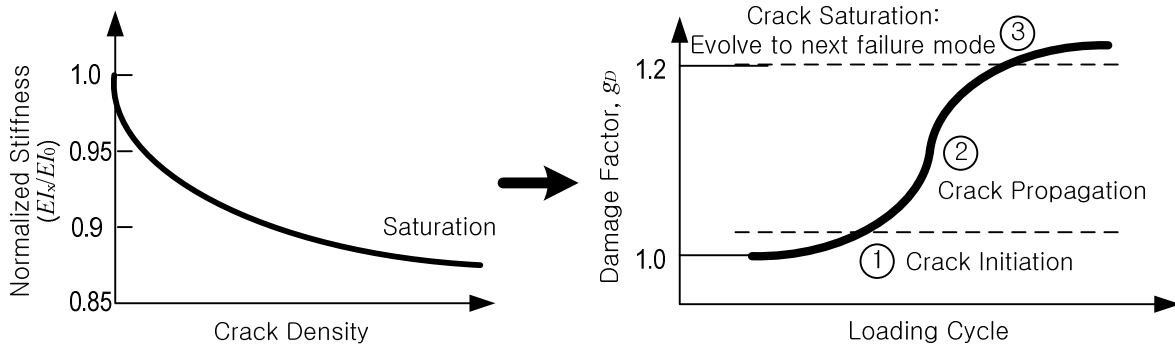


**Figure 5 Stiffness Reduction Model (L)<sup>20</sup>, Simple Damage Model for the Matrix Cracking (R)**

## B. Triple Redundancy Fault Detection

As described in the background section, there is limited vibrational power that can be harvested. In particular, for the range of wind conditions and turbine sizes studied in Ref. 15, the maximum available power  $P_{avail}$  is no more than  $30 \text{ W/m}^3$  even under the most favorable operating conditions. Given current energy harvester efficiencies, it would take approximately 4 minutes to store sufficient energy to wirelessly transmit a single pulse. Additional energy would be required to take a strain or accelerometer measurement. As a consequence, it is not possible to use *high sample rate* SHM algorithms with sensors powered by a vibrational energy harvester.

The essential idea of the proposed health monitoring algorithm is to compare identical measurements from the three individual blades. Specifically, the transmission time intervals from the sensing nodes at identical locations on the three turbine blades is compared. This transmission time interval between pulses is a direct measurement of the rate of harvested power. An individual timing measurement is then deemed “unhealthy” if it differs from the remaining blades by more than a specified threshold. The hypothesis is that a damaged blade will yield a sufficiently different measurement than a healthy blade. This triple redundant design is model-free and is commonly used in the aerospace industry<sup>21-23</sup> to achieve high levels of reliability. The triple redundancy enables detection of a single blade failure because the failed blade yields outlier measurements in comparison to the two healthy blades. This approach relies on three key assumptions. First, it is assumed that the three blades are initially healthy. Second, it is assumed that two or more blades do not fail in the same way at the same location. Third, the three blades are assumed to have similar wind loading conditions when averaged over time. In the case of matrix cracking, higher available power  $P_{avail}$  leads to a shorter transmission time interval. In this way, the damage can be detected with low sampling frequency because the speed of damage progression is much slower than the sampling period.

**Eq. (11)** is the general relation that can be used to model the time between pulse transmissions for any strain history and damage profile. The important point is that the time to charge the harvester for a pulse transmission depends on several factors including the harvester properties, installation configuration and loading conditions. For example, variations in the wind speed will change the vibrational energy  $P_{avail}$  and hence the timing of the pulses from energy harvesting sensors. However, it is assumed that all three blades operate in the same wind conditions. Hence, changes in wind conditions should lead to similar changes in the pulse time of the energy harvesting sensors located on all blades. Thus it is useful to define a non-dimensional ratio to compare the pulse timings from each energy harvester. Let  $\Delta t_i(t)$  denote the time difference between two most recent pulses received at time  $t$  from blade  $i$ . The time differences computed from harvesters on blades 1, 2, and 3 can be compared at time  $t$  using the following three ratios:

$$R_{1-2}(t) = \frac{\Delta t_1(t)}{\Delta t_2(t)}, R_{1-3} = \frac{\Delta t_1(t)}{\Delta t_3(t)}, R_{2-3} = \frac{\Delta t_2(t)}{\Delta t_3(t)}. \quad (14)$$

The use of non-dimensional ratios minimizes the effect of exogenous influences, e.g. wind conditions, thus enabling blade damage to be more easily detected in the processed data. The pulse ratios may not be unity even if all blades are healthy, i.e. blade timings can be different due to differences in sensor installation, individual harvester efficiency, etc. However, matrix cracking on a single blade will lead to higher available power  $P_{avail}$  and hence a shorter transmission time interval. Damage can be detected over time by noting that the transmission time ratios for a single blade will diverge from the initial values. For example, damage in blade 3 will cause more frequent transmissions and thus shorter transmission time intervals. As a result the ratios computed using blade 3, i.e.  $R_{2,3}$  and  $R_{3,1}$ , will diverge from their initial values. Deviations sufficient to indicate blade damage can be detected by a simple threshold. The precise implementation is as follows. First, an initial dataset is recorded under the assumption that each blade is healthy. The transmission time ratios  $R_{i,j}(t)$  ( $i, j=1,2,3$  and  $j \neq i$ ) obtained from this initial dataset are averaged in time to obtain the constant ratio  $\bar{R}_{i-j}$  that corresponds to healthy operation. Damage is detected on blade  $i$  ( $=1,2,3$ ) if  $|R_{i-j}(t) - \bar{R}_{i-j}| > T$  for  $j \neq i$  where  $T$  is the detection threshold. This proposed detection method is evaluated in the next section using experimental strain data from a utility-scale turbine combined with the model to simulate the harvester in both healthy and unhealthy conditions.

#### IV. Results and Discussion

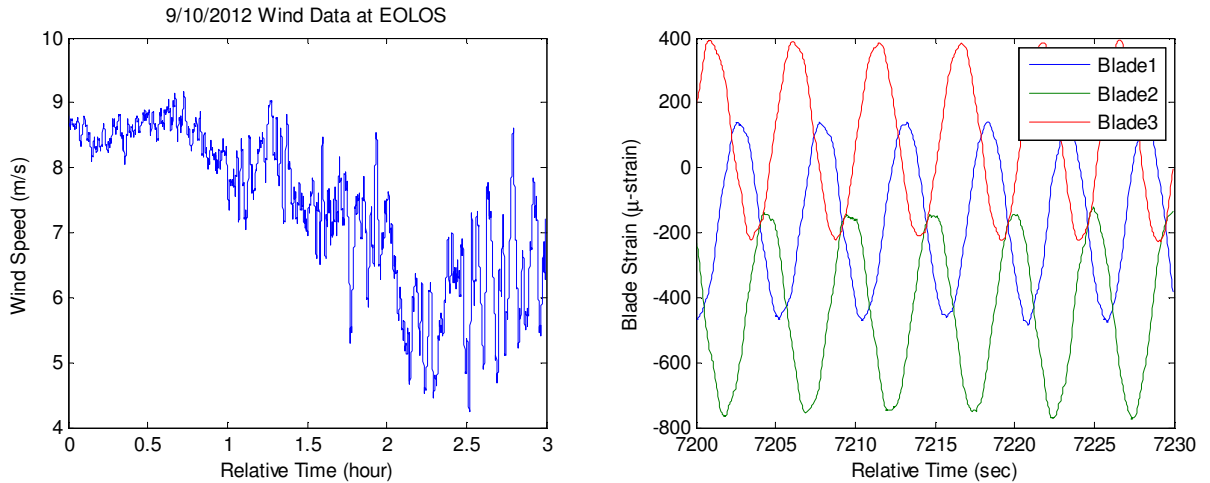


**Figure 6** Wind Data (L), Edgewise Strain Data from Leading Edge of Three Blades at the Root (R)

##### A. Eolos Wind Turbine

The Eolos<sup>24</sup> Wind Energy Research consortium was established in 2010 by the University of Minnesota and includes the Wind Research Field Station located at the University of Minnesota's UMore Park facility. In the summer of 2011, a state-of-the-art 2.5MW C96 Clipper Liberty Wind Turbine<sup>25</sup> was installed at UMore Park. The turbine has a rotor diameter of 96 meters and tower hub height of 80 meters. The turbine includes fiber optic strain gages and accelerometers installed at various points on the three blades and tower base for research purposes. In addition, a 130 m tall meteorological tower, located upwind of the turbine, is instrumented with an array of advanced wind measurement technologies including sonic anemometers, temperatures sensors and cameras. All data

collected at the site, including the turbine, blade, foundation, and met tower are transmitted back to the university campus through high-speed internet for real-time viewing and sharing. Blade strain and wind data (obtained from an upstream met tower) from the Eolos turbine are used in this paper to evaluate the proposed health monitoring algorithm. For each blade, strain at up to 10 locations is continuously recorded at a frequency of 20 Hz. Wind data and turbine operating conditions, sampled at 1 Hz, are recorded and time stamped to correspond to the strain data. An example of data obtained from the Liberty turbine at the Eolos Field Station is shown in **Figure 6**. It shows data recorded for three hours on September 10<sup>th</sup>, 2012 (left) and magnified strain data for 30 seconds of the same day (right). Strain data are from three strain gages at the same locations (root leading edge) of three blades. As shown, strain values of each measurement are asynchronously periodic and they have dissimilar non-zero means.

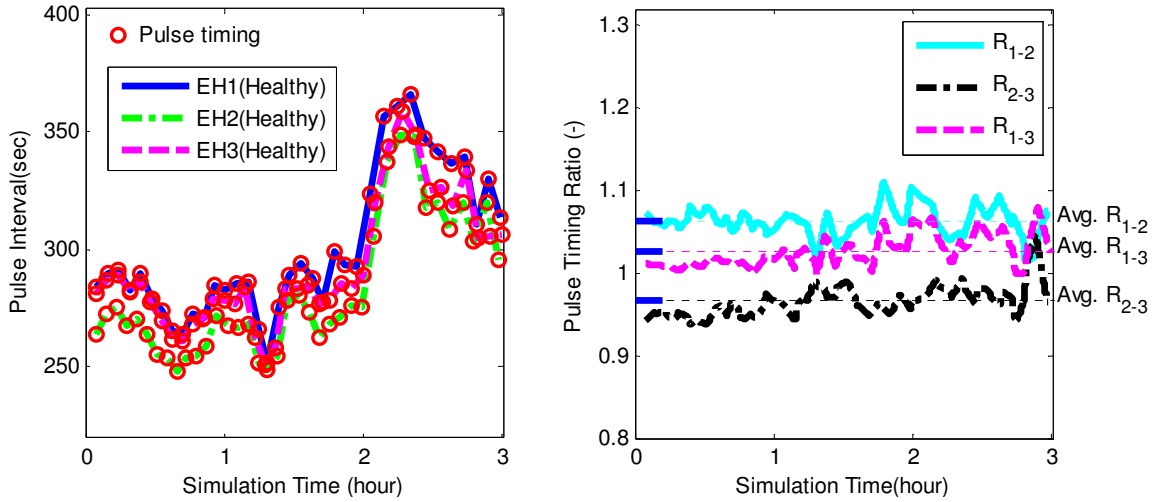


**Figure 7 Pulse Timing of EHs (L), Ratio Factors of EHs (R)**

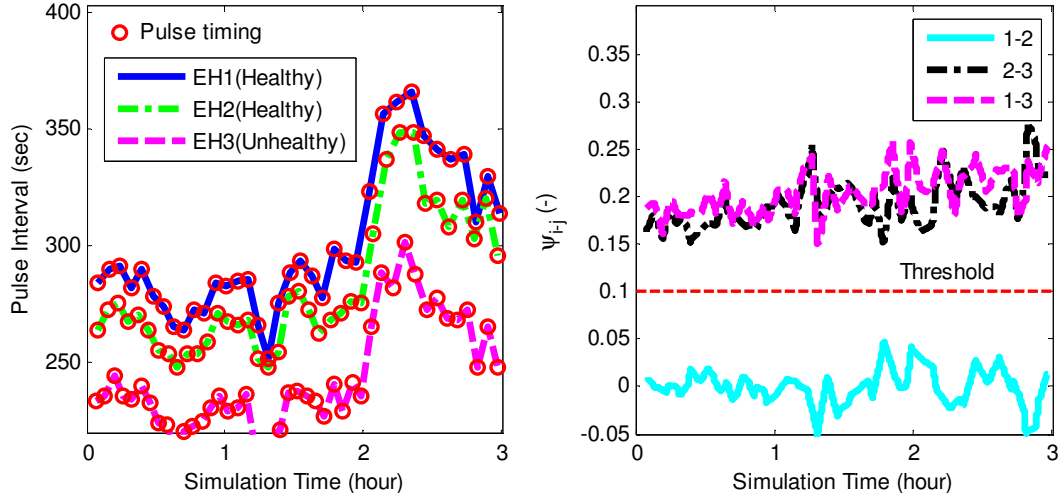


**Figure 8 Unhealthy Blade Simulation: Pulse Timing of EHs (L), Ratio Factors of EHs (R)**

## B. Data Process using a Ratio Factor (Healthy Blades)

We expect the Eolos turbine blades to be “healthy” since the turbine has only recently been installed. Hence the data in **Figure 6** represent healthy blades. The EH is modeled after the properties of the M2814P2 MFC which has a design factor of  $K_{EH}$  is  $14.27 \text{ mm}^3$ . The signal pulse timing, shown in **Figure 7** (left), was generated using the logged data shown in **Figure 6** and a model of this EH. It is noted that the pulse timing interval increases after  $t \approx 2$  hour due to the decrease in wind speed after  $t \approx 1$  hour. The trends of three EHs pulse timings are similar despite this variation in the working condition. **Figure 7** (right) shows the three ratios defined in **Eq. (14)**. This figure shows that the ratios remain relatively constant in spite of the variations and DC offsets in the strain measurements. In effect the long charging time ( $\sim 600$  seconds here) averages out the short term variations and the signal DC offsets do not cause variations in the time interval ratios. As discussed above, the pulse timings may not be equal for each EH



and hence the timing ratios are not equal to unity. The transmission time ratios shown in the right subplot of **Figure 7** were averaged to obtain the nominal ratios  $\bar{R}_{i-j}$  that corresponds to healthy operation.

### C. SHM Simulation for a Unhealthy Blade

After certain cycles of fatigue loading, cracks are saturated and  $g_D$  becomes some higher number than 1.0. This subsection considers the damage model in **Figure 5** (right). A stage 3 cracking (saturation) damage is simulated in blade 3. This is simulated by changing the blade 3 damage factor in **Eq. (11)** from its nominal value ( $g_D = 1.0$ ) to a value corresponding to 20% increase in harvested energy ( $g_D = 1.2$ ). The damage would typically occur over a long time scale and hence the damage factor is assumed to be constant on the time-scale of the simulation results shown here. The strain data shown in **Figure 6** is again used to simulate the harvester pulse timings for the healthy blades ( $i=1,2$ ) and unhealthy blade ( $i=3$ ). The left subplot of **Figure 8** shows the simulated pulse timings. The pulse timings for blade 3 have deviated from the healthy values shown in **Figure 7**. However, the damage signal is not easily discernable due to the variations in pulse intervals. The three ratio factors  $R_{i-j}$  are computed and then subtracted from the averaged initial values to obtain the deviations from healthy signals:  $\psi_{i-j}(t) := R_{i-j}(t) - \bar{R}_{i-j}$ . These deviations are shown in the right subplot of **Figure 8**. It is clear from this figure that the ratios computed with blade 3 deviate significantly and consistently from the healthy values. A threshold, chosen as  $T=1.1$ , can be used to distinguish between small (healthy) values and larger (unhealthy) values. Further investigation is needed to understand the appropriate threshold level to balance the detection and false alarm rate of the proposed algorithm.

## V. Conclusion

This paper described a structural health monitoring (SHM) algorithm to detect damage in wind turbine blades. The system relies on an accumulated energy sensor that harvests low frequency vibrational energy from the blade and wirelessly transmits a pulse once sufficient energy has been stored. The premise of this sensing approach is that the timing of signal transmissions is indicative of the structural health. The SHM algorithm identifies damage by comparing the transmission timing of sensors installed at the same location on the three blades. The effectiveness of the SHM algorithm was evaluated using experimental strain data from a 2.5MW turbine combined with a model of the energy harvester. These results indicate that simulated damage corresponding to approximately 20% increase in harvested energy can be detected by the proposed SHM algorithm. Future work will investigate the details of the algorithm including the threshold selection. In addition, more accurate damage models will be used to understand how the distance between the damage and sensor locations impacts the detection performance.

## Appendix

Consider an EH that is excited by a single dominant harmonic function with frequency  $f$  and peak amplitude (mean to peak) strain  $\varepsilon_a$  (unitless):  $\varepsilon(t) = \varepsilon_a \sin(2\pi ft)$ . Input strain energy of one cycle  $w_{in}^{(1)}$  can be calculated based on **Eq. (4)**

$$w_{in}^{(1)} = E\varepsilon_a^2 2\pi f \left( \int_0^{\frac{1}{2f}} \sin 2\pi ft \cdot \cos 2\pi ft dt + \int_{\frac{1}{2f}}^{\frac{3}{2f}} \sin 2\pi ft \cdot \cos 2\pi ft dt \right) = 2 \cdot \frac{1}{2} E\varepsilon_a^2. \quad (\text{A1})$$

Given the excitation frequency  $f$  and the total time of excitation  $\delta t$ , then the number of excitation cycles  $n$  is

$$n = f \cdot \delta t. \quad (\text{A2})$$

Combining **Eqs. (A1, A2)**, the strain energy input for  $n$  cycles  $w_{in}^{(n)}$  is

$$w_{in}^{(n)} = n \cdot 2 \cdot \frac{1}{2} E\varepsilon_a^2 = f \delta t \cdot E\varepsilon_a^2. \quad (\text{A3})$$

The amount of harvested energy  $w_{EH}$ , including EH efficiency  $\eta$ , is

$$w_{EH} = \eta E \cdot \varepsilon_a^2 f \cdot \delta t. \quad (\text{A4})$$

## Acknowledgments

This work was supported by the University of Minnesota Institute on the Environment, IREE Grant No. RS-0029-12 entitled "Development of self-powered wireless sensor for structural health monitoring in wind turbine blades." This work was also partially supported by the National Science Foundation under Grant No. NSF-CMMI-

1254129 entitled "CAREER: Probabilistic Tools for High Reliability Monitoring and Control of Wind Farms." Any opinions, findings, and conclusions or recommendations expressed in this paper are those of the authors and do not necessarily reflect the views of the NSF. And the authors would like to thank Dr. Rusen Yang for his helpful advice regarding the Energy Harvester capability.

## References

- <sup>1</sup>Swisher, R., "Keys to Achieving 20 Percent Wind by 2030," *Cogeneration and Distributed Generation Journal*, Vol. 24, No. 3, 2009, pp. 66-77.
- <sup>2</sup>Ghoshal, A., Sundaresan, M.J., Schulz, M.J., "Structural health monitoring techniques for wind turbine blades," *Journal of Wind Engineering and Industrial Aerodynamics*, Vol. 85, No. 3, 2000, pp. 309-324.
- <sup>3</sup>Khan, M.M., Iqbal, M.T., and Khan, F., "Reliability and condition monitoring of a wind turbine," *IEEE*, 2005, pp. 1978-1981.
- <sup>4</sup>Paquette, J., Hughes, S., van Dam, J., "Fatigue Testing of 9 m Carbon Fiber Wind Turbine Research Blades," *46th AIAA Aerospace Sciences Meeting and Exhibit, Reno, NV*, 2008.
- <sup>5</sup>Carden, E.P., and Fanning, P., "Vibration based condition monitoring: a review," *Structural Health Monitoring*, Vol. 3, No. 4, 2004, pp. 355-377.
- <sup>6</sup>White, J., Adams, D., Rumsey, M., "Impact loading and damage detection in a carbon composite TX-100 wind turbine rotor blade," 2008.
- <sup>7</sup>Deines, K., Marinone, T., Schultz, R., "Modal Analysis and SHM Investigation of CX-100 Wind Turbine Blade," *Rotating Machinery, Structural Health Monitoring, Shock and Vibration, Volume 5*, 2011, pp. 413-438.
- <sup>8</sup>Rumsey, M.A., and Paquette, J.A., "Structural health monitoring of wind turbine blades," *The 15th International Symposium on: Smart Structures and Materials & Nondestructive Evaluation and Health Monitoring*, International Society for Optics and Photonics, 2008, pp. 69330E-69330E-15.
- <sup>9</sup>Ciang, C.C., Lee, J.R., and Bang, H.J., "Structural health monitoring for a wind turbine system: a review of damage detection methods," *Measurement Science & Technology*, Vol. 19, No. 12, 2008.
- <sup>10</sup>Schulz, M.J., Sundaresan, M.J., and National Renewable Energy Laboratory (U.S.), "Smart sensor system for structural condition monitoring of wind turbines, May 30, 2002 - April 30, 2006," Vol. 2011, National Renewable Energy Laboratory, Golden, Colo., 2006, pp. viii, 43 p.
- <sup>11</sup>Montalvao, D, Maia, "A review of vibration-based structural health monitoring with special emphasis on composite materials," Vol. 38, Sage, Thousands Oaks, CA, ETATS-UNIS, 2006, pp. 30.
- <sup>12</sup>Light-Marquez, A., Sobin, A., Park, G., "Structural Damage Identification in Wind Turbine Blades Using Piezoelectric Active Sensing," *Structural Dynamics and Renewable Energy, Volume 1*, 2011, pp. 55-65.
- <sup>13</sup>Pitchford, C.W., "Impedance-based structural health monitoring of wind turbine blades," 2007.
- <sup>14</sup>Zayas, J.R., Paquette, J., and Werlink, R.J., "Evaluation of NASA PZT Sensor/Actuator for Structural Health Monitoring of a Wind Turbine Blade," Vol. 1020, 2007.
- <sup>15</sup>Lim, D.-W, Mantell, S.C., and Seiler, P.J., "Wind Turbine Blades as a Strain Energy Source for Energy Harvesting." *AIAA 51st Aerospace Sciences Meeting, Grapevine Texas*, 2013, pp. 0449-0457.
- <sup>16</sup>Jonkman, J.M., and Buhl Jr, M.L., "FAST user's guide," *Rep. no. NREL/EL-500-38230, NREL, Golden, Colorado, USA*, 2005.
- <sup>17</sup>Microstrain, inc., Strain Energy Harvesting for Wireless Sensor Networks, <http://www.microstrain.com/energy-harvesting/eh-link>. [cited 05 June 2013]
- <sup>18</sup>Smart Materials Corp, <http://www.smart-material.com/MFC-product-main.html>. [cited 05 June 2013]
- <sup>19</sup>Adams, D.E., "Health monitoring of structural materials and components," *Methods with Applications*. Wiley, New York, 2007.
- <sup>20</sup>Pawar, P.M., and Ganguli, R., "Modeling progressive damage accumulation in thin walled composite beams for rotor blade applications," *Composites Science and Technology*, Vol. 66, No. 13, 2006, pp. 2337-2349.
- <sup>21</sup>Yeh, Y., "Triple-triple redundant 777 primary flight computer," *Aerospace Applications Conference, 1996. Proceedings., 1996 IEEE*, Vol. 1, IEEE, 1996, pp. 293-307.
- <sup>22</sup>Yeh, Y., "Safety critical avionics for the 777 primary flight controls system," *Digital Avionics Systems, 2001. DASC. 20th Conference*, Vol. 1, IEEE, 2001, pp. 1C2/1-1C2/11 vol. 1.
- <sup>23</sup>Collinson, R. PG, "Introduction to Avionics Systems," 2003
- <sup>24</sup>Eolos Wind Energy Reserach Consortium, <http://www.eolos.umn.edu>. [cited 05 June 2013]
- <sup>25</sup>The Liberty 2.5 MW Wind Turbine: Clipper Design. <http://www.clipperwind.com>. [cited 05 June 2013]